



Citation for published version:

Ma, Y, Domingo-Félez, C, Plósz, BG & Smets, BF 2017, 'Intermittent Aeration Suppresses Nitrite-Oxidizing Bacteria in Membrane-Aerated Biofilms: A Model-Based Explanation', *Environmental Science and Technology*, vol. 51, no. 11, pp. 6146-6155. <https://doi.org/10.1021/acs.est.7b00463>

DOI:

[10.1021/acs.est.7b00463](https://doi.org/10.1021/acs.est.7b00463)

Publication date:

2017

Document Version

Peer reviewed version

[Link to publication](#)

This document is the Accepted Manuscript version of a Published Work that appeared in final form in *Environmental Science and Technology*, copyright © American Chemical Society after peer review and technical editing by the publisher. To access the final edited and published work see <https://doi.org/10.1021/acs.est.7b00463>.

University of Bath

General rights

Copyright and moral rights for the publications made accessible in the public portal are retained by the authors and/or other copyright owners and it is a condition of accessing publications that users recognise and abide by the legal requirements associated with these rights.

Take down policy

If you believe that this document breaches copyright please contact us providing details, and we will remove access to the work immediately and investigate your claim.

1 Intermittent Aeration Suppresses Nitrite-Oxidizing Bacteria
2 in Membrane-Aerated Biofilms

3 *Yunjie Ma, Carlos Domingo-Félez, Benedek G. Plósz,[†] and Barth F. Smets**

4

5 Department of Environmental Engineering, Technical University of Denmark, Miljøvej Building 113, 2800
6 Kongens Lyngby, Denmark.

7

8 * Corresponding Author: E-mail: bfsm@env.dtu.dk, Tel: +45 4525 1600 Fax: +45 4593 2850

9 [†]Present Address: Department of Chemical Engineering, University of Bath, Claverton Down, BA2
10 7AY Bath, United Kingdom.

11 **Abstract**

12 Autotrophic ammonium oxidation in membrane-aerated biofilm reactors (MABRs) can make treatment of
13 ammonium-rich wastewaters more energy-efficient, especially within the context of short-cut ammonium
14 removal. The challenge is to exclusively enrich ammonium-oxidizing bacteria (AOB). To achieve nitrification,
15 strategies to suppress nitrite-oxidizing bacteria (NOB) are needed, which are ideally grounded on an
16 understanding of underlying mechanisms. In this study, a counter-diffusion nitrifying biofilm reactor was
17 operated under intermittent aeration. During eight months operation, AOB dominated, while NOB were
18 suppressed. Based on dissolved oxygen (DO), ammonium (NH_4^+), nitrite (NO_2^-) and nitrate (NO_3^-) profiles
19 within the biofilm and in the bulk, a 1-dimensional nitrifying biofilm model was developed and calibrated.
20 The model was utilized to explore the potential mechanisms of NOB suppression associated with intermittent
21 aeration, considering DO limitation, direct pH effects on enzymatic activities, and indirect pH effects on
22 activity via substrate speciation. The model predicted strong periodic shifts in the spatial gradients of DO,
23 pH, free ammonia and free nitrous acid, associated with aerated and non-aerated phases. NOB suppression
24 during intermittent aeration was mostly explained by periodic inhibition caused by free ammonia due to
25 transient periodic pH upshifts. Dissolved oxygen limitation did not govern NOB suppression. Different
26 intermittent aeration strategies were then evaluated for nitrification success in intermittently aerated MABRs:
27 both aeration intermittency and residual free ammonia turned to be effective control parameters.

28

29 **Introduction**

30 Short-cut ammonium (NH_4^+) removal via nitrite (NO_2^-) is more energy- and cost- efficient than traditional
31 NH_4^+ removal via nitrate (NO_3^-) due to reduced aeration and external electron donor requirements.^{1,2,3} This
32 process requires full nitrification (oxidation of all NH_4^+ to NO_2^-) and zero nitrification (oxidation of none of the
33 NO_2^- to NO_3^-); in other words minimal activity of nitrite-oxidizing bacteria (NOB) and maximal activity of
34 ammonium-oxidizing bacteria (AOB). Similar conditions– with only partial nitrification– can also be exploited
35 to convert NH_4^+ to a 50:50 mixture of NO_2^- and NH_4^+ , which can then be coupled to anoxic NH_4^+ oxidation
36 to attain even more resource efficient ammonium removal.^{4,5}

37 Various conditions have been successfully tested to suppress NOB over AOB activity or wash-out NOB over
38 AOB biomass to attain nitrification in suspended growth systems. They include the operation of bioreactors at
39 limited dissolved oxygen (DO) concentrations,⁶ at high temperature combined with low solids retention
40 times,¹ and at elevated free ammonia (FA) and/or free nitrous acid (FNA) concentrations.⁷ In all cases NOB
41 suppression or outcompetition versus AOB is based on differential growth kinetics. Sometimes, the proper
42 choice of system inoculum also accelerates AOB over NOB selection.⁸ By contrast, maintaining long-term
43 nitrification in biofilm-based reactors can be more challenging⁹ due to long solids retention times in biofilms
44 that interfere with outcompetition based on kinetic principles. Finding operational conditions and confirming
45 mechanisms that suppress NOB in biofilms remains a challenge. On the one hand, the existence of strong
46 spatial chemical gradients (e.g. of DO, pH and nitrogenous species) in nitrifying biofilms¹⁰ makes it difficult
47 to prescribe environmental conditions that favor AOB over NOB in the system. On the other hand, the
48 existence of multiple simultaneous chemical gradients complicates identification of the underlying
49 mechanism(s) that suppresses NOB. For example, pH and DO gradients occur simultaneously in active
50 nitrifying biofilms:¹¹ it is difficult to unravel to what extent nitrification failure or success is associated with
51 the differential effect of oxygen (AOB and NOB having different oxygen affinities)¹² or the differential
52 effects of pH (AOB and NOB responding differently to pH– as a consequence of the pH-dependent
53 maximum growth rates^{13,14} and the pH-dependent speciation of FA and FNA which act as both substrates and
54 inhibitors).

55 Mathematical models are one way to describe multiple processes that occur simultaneously in time and space
56 in nitrifying biofilms.^{15,16} A multi-species nitrifying biofilm model (MSNBM) was explicitly developed to
57 study the competition between AOB and NOB; effects of DO, pH, FA and FNA on growth kinetics were
58 incorporated in a spatially explicit way to evaluate operational conditions for NOB suppression in co-
59 diffusion biofilms.^{3,17} Park et al.¹⁷ showed that FA inhibition of NOB was more efficient in nascent biofilms
60 (when residual NH_4^+ was still high), but that DO limitation was the dominant mechanism of NOB
61 suppression in established biofilms. Besides bulk DO and influent NH_4^+ concentration, the model suggested
62 that bulk buffer capacity was another means to manipulate NOB suppression by affecting pH gradients
63 within biofilms.

64 While AOB/NOB competition in conventional co-diffusion biofilms has been studied in some detail,^{3,17,18}
65 there are less studies on AOB/NOB competition in the context of nitrification in counter-diffusion biofilms.
66 Counter-diffusion biofilms develop in membrane-aerated biofilm reactors (MABRs), where air delivery is
67 via the biofilm base.¹⁹ MABRs have been broadly explored for autotrophic N removal.^{11,20,21} In counter-
68 diffusion nitrifying MABRs, active bacteria thrive at the base of the biofilm, where they utilize oxygen
69 supplied from the membrane lumen. Growth of bacteria- including NOB- at the biofilm base would limit the
70 chance for outcompetition, once established, due to spatial protection by the overlying biofilm layers.
71 Efficient operation of MABRs to attain long-term nitrification has, to our knowledge, not been documented,
72 with the exception of one, highly-loaded (33 g-N/m²/day) fully NH_4^+ penetrated MABR where controlling
73 DO concentrations at the membrane-biofilm interface sufficed to maintain nitrification.²²

74 Recently, Pellicer-Nàcher et al.²¹ observed that fully nitrification MABRs accumulated NO_2^- immediately after
75 switching from continuous to intermittent aeration, even at elevated oxygen loadings. The causal link
76 between nitrification onset and aeration regime change were not explored. Here we report additional
77 experimental evidence of NOB suppression in intermittently aerated MABRs and we develop and calibrate
78 an improved MSNBM incorporating explicit pH calculation. Using the calibrated model, we systematically
79 evaluate potential causes for NOB suppression associated with intermittent aeration. From this analysis, we
80 identify the periodic FA inhibition- caused by transient pH upshifts and decreases at the biofilm base- as the

81 likely key cause for NOB suppression. A suitable operational window for an effective nitrification control in
82 counter-diffusion systems is finally proposed.

83 **Materials and Methods**

84 **2.1 Reactor Operation and Measurement Methods**

85 **Reactor Configuration and Operation**

86 The counter-diffusion MABRs consisted of two tubular gas filled PDMS membranes (3100506, Labmarket,
87 Germany), both fixed in parallel to its longer dimension (Figure S1). The system had a liquid volume of 0.83
88 L (reactors: 31.5×5×3.5 cm) and was inoculated with enriched nitrifying biomass.²¹ To start up the system,
89 the reactor was first run in a batch mode with an initial NH_4^+ concentration at 300 mg-N/L and continuous
90 aeration. The onset of NH_4^+ consumption without oxygen accumulation in the bulk suggested biomass
91 attachment around the membranes. Subsequently, the MABR was operated in continuous flow mode under
92 intermittent aeration. Synthetic wastewater was fed continuously with an NH_4^+ concentration at 75 mg-N/L
93 and without external organic carbon. Hydraulic retention time was 12 hours. The intermittent aeration
94 strategy consisted of a 6-hour aeration period (100% air) followed by a 6-hour non-aeration period (100%
95 N_2). The aeration cycles were controlled by a set of solenoid valves and the pressure in the lumen was 35
96 kPa. The bulk phase was completely mixed by recirculating at 1.5 L/min. DO and pH were measured with
97 electrodes in the recirculation line (CelloX 325 and Sentix 41, WTW, Germany). Bulk pH was not
98 controlled and remained at 7.2 ± 0.2 due to adequate buffer capacity (molar ratio in the influent: $\text{HCO}_3^-/\text{NH}_4^+$
99 = 2.1). Reactor temperature was at $32.5 \pm 0.7^\circ\text{C}$, which was above ambient temperature due to the
100 unintentional heat added by the recirculation pump. N concentrations (NH_4^+ , NO_2^- and NO_3^-) were measured
101 with colorimetric test kits (Spectroquant 14776, 00683, 09713; Merck, Germany).

102 **Microelectrode Measurements**

103 Commercially available DO microelectrode (OX-10, Unisense, Denmark) and lab-made potentiometric
104 microelectrodes for NH_4^+ , NO_2^- and NO_3^- ²³ were used for in-situ profiling measurements within the biofilm.
105 Profiling measurements were performed after biofilms reaching steady state. Microelectrodes were

106 controlled by a motorized micromanipulator to a precision up to 10 μm , and began from the top of the
 107 biofilm. During measurements, the influent and recirculation were kept unchanged. For each profile,
 108 replicates ($n > 3$) were made and the average was considered in model fitting. Besides calibration following
 109 the protocols, the signal drift of N-species sensors over time was corrected by measuring N concentrations
 110 from effluent before and after profiling.

111 2.2 Model Development

112 The MSNBM is a one-dimensional model based on Terada et al.,²⁴ incorporating additional explicit pH
 113 calculation (Table S1). It was implemented in AQUASIM V2.1 with two compartments: a completely mixed
 114 gas compartment and a biofilm compartment containing biofilm and bulk liquid.²⁵ In the counter-diffusion
 115 regime, a physical diffusion link connects the gas compartment to the base of the biofilm, defined as

$$116 \quad A \cdot k_{M,i} \left(\frac{1}{H_i} C_{i,air} - C_{i,base} \right) \quad (1)$$

117 where $C_{i,air}$ and $C_{i,base}$ are concentrations of carbon dioxide (CO_2) or oxygen (O_2) in the gas compartment and
 118 at the biofilm base (mg/L), H is the non-dimensional Henry's Law coefficient (1.32 for CO_2 , 34.55 for O_2 ,
 119 33 $^\circ\text{C}$), $k_{M,i}$ is the silicone membrane gas mass transfer coefficient ($k_{M,\text{O}_2} = 6$ m/d, $k_{M,\text{CO}_2} = 0.8$ m/d, Table S3).
 120 Gas transfer of N_2 and NH_3 are not modeled. Other major modeling assumptions- regarding biofilm structure,
 121 diffusion mass transfer and boundary layer thickness are as in Terada et al.²⁴ Process rate expressions are
 122 shown (Table S2). The calibrated nitrification model incorporating pH is available from the corresponding
 123 author.

124 Biological Processes

125 The MSNBM includes 3 active microbial groups- AOB, NOB, heterotrophs (HB) and inerts accumulated
 126 during decay processes. For the two-step nitrification process, FA and FNA are considered as true substrates
 127 for growth and inhibition in nitritation and nitrataion.²⁶ The growth rate expressions are described as follows,

$$128 \quad \text{AOB: } \mu_{AOB} \cdot X_{AOB} \cdot \frac{S_{O_2}}{K_{O_2}^{AOB} + S_{O_2}} \cdot \frac{S_{FA}}{K_{FA}^{AOB} + S_{FA} + S_{FA} \cdot S_{FA} / K_{I,FA}^{AOB}} \cdot \frac{K_{I,FNA}^{AOB}}{K_{I,FNA}^{AOB} + S_{FNA}} \quad (2)$$

$$129 \quad \text{NOB: } \mu_{NOB} \cdot X_{NOB} \cdot \frac{S_{O_2}}{K_{O_2}^{NOB} + S_{O_2}} \cdot \frac{S_{FNA}}{K_{FNA}^{NOB} + S_{FNA} + S_{FNA} \cdot S_{FNA} / K_{I,FNA}^{NOB}} \cdot \frac{K_{I,FA}^{NOB}}{K_{I,FA}^{NOB} + S_{FA}} \quad (3)$$

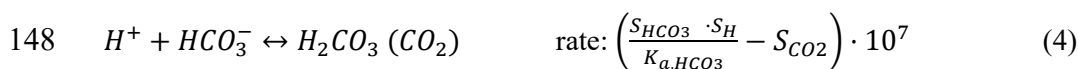
130 where μ is the specific growth rate coefficient (1/day), dependent on local pH and μ_{max} ; S_{O_2} , S_{FA} and S_{FNA}
 131 are O_2 , FA and FNA concentrations (mg/L), respectively; K_{O_2} , K_{FA} and K_{FNA} are half-saturation coefficients
 132 (mg/L); $K_{I,FA}$ and $K_{I,FNA}$ are inhibition coefficients (mg/L). Growth substrate inhibitions (FA for AOB, FNA
 133 for NOB) are incorporated with the Andrews equation. Other inhibitions (FA for NOB, FNA for AOB) are
 134 described with a noncompetitive inhibition term.

135 For the denitrification process, NO_2^- and NO_3^- are modeled as separate electron acceptors. To avoid
 136 unnecessary complexity and focus on AOB/NOB competition, no intermediates (NO or N_2O) are considered.
 137 Bacteria have different decay rates in aeration and non-aeration periods: to simplify the model, AOB/NOB
 138 are assumed not to decay under anoxic or anaerobic conditions,²⁷ meanwhile, HB decay is modified by an
 139 anoxic reduction factor during non-aeration periods.

140 **Chemical Process: pH Calculation**

141 The one-dimensional model can keep track of local pH changes perpendicular to the membrane substratum.
 142 pH along biofilm depth is calculated based on the proton production via nitrification and consumption via
 143 denitrification, the equilibrium reaction with bicarbonate buffer, and CO_2 stripping to the membrane lumen.
 144 The consumption of inorganic carbon for autotrophic growth is neglected as it has insignificant influence on
 145 pH changes under conditions when inorganic carbon is not limiting.

146 Protons produced and consumed in bioprocesses are listed in the stoichiometry matrix. The acid-base
 147 balance reaction with bicarbonate buffer is assumed to occur much faster than biological processes.²⁸



149 where S_H , $S_{HCO_3^-}$ and $S_{H_2CO_3(CO_2)}$ are concentrations of proton, bicarbonate and the sum of carbonic acid and
 150 dissolved carbon dioxide, respectively ($\mu\text{mol/L}$); K_{a,HCO_3} is the dissociation equilibrium constant of carbonic
 151 acid ($0.574 \mu\text{mol/L}$, 33 °C, 1 atm). Protons produced in the nitrification process titrate HCO_3^- to H_2CO_3 , and
 152 over-saturated CO_2 diffuses from the biofilm base to the membrane lumen (Equation 1). Acid-base reactions
 153 with phosphate ions were minor and neglected, as the molar ratio of $H_2PO_4^-/HCO_3^-$ in influent was lower
 154 than 3%.

155 **Limitations/Inhibitions of AOB/NOB Activity**

156 The growth rate expressions of AOB and NOB consider DO and pH effects. DO limitation is assessed by
157 oxygen affinity constants. Two pH effects are included. (1) pH-enzyme effect: pH can affect nitrifying
158 activity directly by changing the enzyme reaction mechanism or increasing the demand for maintenance
159 energy.^{28,29} A Gaussian bell-shaped curve is chosen to model the pH-enzyme dependency of specific growth
160 rates.¹³

$$161 \quad \mu = \frac{\mu_{max}}{2} \left\{ 1 + \cos \left[\frac{\pi}{\omega} \cdot (pH - pH_{opt}) \right] \right\} \quad |pH - pH_{opt}| < \omega \quad (5)$$

162 where μ_{max} is the maximum specific growth rate at the optimal pH- pH_{opt} , ω is the pH range within which
163 μ is larger than a half of μ_{max} . (2) pH substrate-speciation effect: local pH values determine FA/FNA
164 speciation from total NH_4^+/NO_2^- . The speciation between ionized/unionized species is assumed at
165 instantaneous equilibrium.³⁰

$$166 \quad S_{FA} = \frac{K_{a,NH_3} \cdot S_{NH_4}}{S_H} \quad S_{FNA} = \frac{S_{NO_2} \cdot S_H}{K_{a,NO_2}} \quad (6)$$

167 where K_{a,NH_3} and K_{a,NO_2} are dissociation equilibrium constants of ammonium and nitrous acid, respectively
168 (0.000794 and 628.96 $\mu\text{mol/L}$ (33 °C, 1 atm)). Substrate-speciation will result in differential degrees of
169 FA/FNA inhibition.

170 **2.3 Sensitivity Analysis and Parameter Estimation**

171 To investigate the most determinant parameters on reactor performance, a sensitivity analysis was performed.
172 Initial values of kinetic parameters were taken from ASMN model.²⁶ The optimal pH ranges for AOB and
173 NOB growth kinetics (pH_{opt} and ω) were from Park et al..¹³ The temperature correction for μ_{max} and b_{max} are
174 from Hao et al..³¹ The MSNBM was first run in continuous aeration with default values for 300 days to
175 achieve a stable nitrifying biofilm. Then a local sensitivity analysis was performed after switching to
176 intermittent aeration- giving individual parameter a 100% value change while all others remained constant.²⁵
177 Reactor performances were evaluated in terms of ammonium removal efficiency (ARE, $\frac{S_{NH_4,in} - S_{NH_4,eff}}{S_{NH_4,in}}$ %),

178 nitrate production efficiency (NaE, $\frac{S_{NO_3,eff}}{S_{NH_4,in}-S_{NH_4,eff}}$ %), nitrification efficiency (NE, $\frac{S_{NO_2,eff}}{S_{NH_4,in}-S_{NH_4,eff}}$ %) and

179 NOB fraction (fNOB, $\frac{NOB}{NOB+AOB}$ %). The normalized sensitivity function is defined as,

$$180 \quad \delta_j = \sqrt{\text{average}(Sens_{i,j}^2)} \text{ and } Sens_{i,j} = p_{i,j} \frac{\Delta y_j}{\Delta p_{i,j}}, \quad (7)$$

181 where δ_j , y_j and $p_{i,j}$ are the sensitivity function, the output reactor performances (ARE, NaE, NE or fNOB),
182 and the input parameters, respectively. $Sens_{i,j}$ was evaluated at different times during the aeration cycles
183 (time interval of 0.01 day) and at 20 equidistant points within the biofilm or 1 point in the bulk phase. The
184 averaged value was considered in the sensitivity analysis and parameter sensitivity was ranked for each
185 targeted performance metric. We focused on biokinetic and stoichiometric parameters related to AOB and
186 NOB, as HB parameters are of secondary importance in nitrifying biofilms.³²

187 The most sensitive parameters were calibrated with steady state experimental data. The model calibration
188 was carried out by trial and error through adjusting the parameter values one by one to minimize the fitting
189 error. Root mean squared error was used to assess the quality of model-data fit as the objective function,

$$190 \quad RMSE = \sqrt{\text{average}(\sum_j \sum_i (\frac{y_{model,i,j} - y_{meas,i,j}}{y_{meas,j,average}})^2)} \quad (8)$$

191 where j is the targeted variable measured or estimated (NH_4^+ , NO_2^- , NO_3^- and DO), i is a sample point along
192 biofilm depth ($i = 20$). The model was validated with additional experimental data from this MABR and
193 experimental data from a separate membrane-aerated biofilm reactor (MABR2) operated under 4 different
194 ammonium surface loadings (Table S5, detailed description of the experimental data used in model
195 calibration and validation).³³ The calibrated parameters were checked by comparing RMSE in the calibration
196 with RMSE in the validation and the Janus coefficient (J) was calculated,³⁴

$$197 \quad J^2 = \frac{RMSE_{val}^2}{RMSE_{cal}^2} \quad (9)$$

198 2.4 Model Simulations

199 The calibrated MSNBM was run in 3 scenarios (Table S6, detailed description of each simulation scenario):

200 (1) To validate the model with extra experimental data, the calibrated MSNBM was ran in intermittent
201 aeration (6-hour aeration period and 6-hour non-aeration period) under different NH_4^+ surface loadings or in
202 continuous aeration in a batch test. Then the determinant factor(s) that govern NOB suppression in this
203 MABR was explored with the validated model.

204 (2) To clarify why NOB suppression occurred after switching to intermittent aeration from continuous
205 aeration, the model was run in continuous aeration to achieve a nitrifying biofilm, then aeration was switched
206 to the same intermittent aeration as scenario 1.

207 (3) To optimize the operational window for nitrification in intermittently aerated MABRs, different
208 intermittent aeration strategies and influent concentrations were simulated in MSNBM after achieving a
209 nitrifying biofilm in continuous aeration. The effects of aeration intermittency and residual NH_4^+ (FA)
210 concentrations on NOB suppression were evaluated.

211 **Results and Discussion**

212 **3.1 Model Calibration and Evaluation**

213 A sensitivity function, considering the sum of reactor performances (ARE, NaE, NE and fNOB), was
214 calculated to rank parameters (Figure S2). The most sensitive parameter is μ_{max}^{AOB} , followed by $K_{I,FA}^{AOB}$, μ_{max}^{NOB} ,
215 $K_{I,FA}^{NOB}$, $K_{O_2}^{AOB}$ and $K_{O_2}^{NOB}$. The ranking shows that μ_{max} is the most determinant among all kinetic parameters in
216 nitrogen conversion simulations. It is consistent with the sensitivity analysis of Wang et al.³² who ranked
217 kinetic parameters in terms of nitrification performance and biofilm development in nitrifying biofilm reactors.
218 The higher sensitivity regarding performance within the biofilm (Figure S2B) versus the bulk (Figure S2A)
219 suggests that in-situ microprofiling data is more informative in model calibration than bulk measurements,
220 which were typically used.^{22,35} Therefore, microprofiling measurements (NH_4^+ , NO_2^- , NO_3^- and DO) in the
221 first aeration hour at steady state were used to calibrate sensitive parameter(s). Microprofiles in the last
222 aeration hour (NH_4^+ , NO_2^- , NO_3^- and DO) and bulk profiles in an intermittent aeration cycle (NH_4^+ , NO_2^- ,
223 NO_3^- , DO and pH) at steady state were used for validation. Additional validation of the model and its
224 parameter estimates was obtained by fitting the initial reactor performance (NH_4^+ , NO_2^- and NO_3^-) when

225 operated in batch start-up mode, and by fitting the biofilm performance (NH_4^+ , NO_2^- , NO_3^- and pH) of a
226 separately operated MABR under different NH_4^+ surface loadings.

227 By fitting the most sensitive parameter- μ_{max}^{AOB} in the reported range,¹² the RMSE decreased to 0.5 and the
228 deviation in NO_3^- fitting contributed the most to the error. Thus, the next most sensitive parameter- μ_{max}^{NOB} - in
229 NO_3^- sensitivity ranking (Figure S3) was added to the calibration and RMSE decreased to 0.1. Values of
230 μ_{max}^{AOB} and μ_{max}^{NOB} were within a reasonable range: the estimated maximum growth rates at the optimal pH were
231 2.35 d^{-1} for AOB and 2.15 d^{-1} for NOB (Table 1). Predicted microprofiles agree with measurements in the
232 first aeration hour at steady state (Figure 1A): NH_4^+ is consumed along biofilm depth and NO_2^- is produced;
233 NO_3^- remains at lower concentrations than NO_2^- within the biofilm; DO penetrates $60 \mu\text{m}$ into the biofilm
234 base. The greatest divergence in the overall fitting corresponds to NO_2^- at the biofilm base (6 mg-N/L) but
235 only overestimates FNA concentrations by 0.002 mg-N/L . Errors in DO fitting at the membrane-biofilm
236 interface (6.6 mg/L predicted versus 1.7 mg/L measured) have a minor influence on the oxygen competition
237 between AOB and NOB (Table S4), consistent with Lackner and Smets³⁶ who reported that oxygen
238 concentrations at interfaces were not decisive in nitrification performance in MABRs. Additionally,
239 uncertainty in measuring the interface DO could be caused by microbial activities on the membrane and an
240 efficiency factor E ($1.3 \sim 4.3$) was suggested to correct measured values.³³

241 MSNBM predicts consistent profiles in the different model validations. It predicted lower NH_4^+ and higher
242 NO_2^- within the biofilm in the last aeration hour (Figure 1B) and uniform dynamic variations of bulk
243 concentrations in a 12-hour intermittent aeration cycle. For example, it captured the pH decreases in the 6-
244 hour aeration phase and increases in the 6-hour non-aeration phase (Figure 1C). It also predicted
245 simultaneous production of NO_2^- and NO_3^- in the batch mode data validation (Figure S4A) and predicted
246 NH_4^+ consumption and NO_2^- production following the tendencies observed in MABR2 (Figure S4B). Janus
247 coefficients were around $1.9 (\pm 0.5)$, showing that the RMSEs were within the same order of magnitude in
248 calibration and validations.

249 **3.2 Model-based Exploration of NOB Suppression in Intermittently Aerated MABRs**

250 NOB suppression is the result of indirect and direct (competitive) interactions between AOB and NOB in the
251 local environment. Net microbial activities are captured in the specific growth rates: biomass types with the
252 higher specific growth rate will win the local competition. In the studied system, oxygen was provided
253 intermittently from membrane lumen. The biomass type with the higher specific growth rate (AOB or NOB)
254 thus dominated the oxygen utilization.

255 Consistent with experimental reactor operations, simulations were initiated with fully-nitrifying biomass and
256 subject to intermittent aeration. Both simulation and experimental data showed that after 2 weeks in
257 intermittent aeration bulk N concentrations became stable, especially NO_3^- was below 1 mg-N/L indicating
258 efficient suppression of NOB activity (Figure S9). To illustrate the competition in the first nitrifying stage,
259 profiles of specific growth rates of AOB and NOB during an aeration cycle (6 hours) are plotted at day 15
260 (Figure 2A). The averaged μ at time intervals shows kinetic variations over time: (1) 0-15 minutes, with the
261 onset of aeration microbial activities recover from the previous non-aeration period and increase
262 dramatically; (2) 15-180 minutes, AOB activity becomes stable, while NOB activity still recovers; (3) 180-
263 360 minutes, both AOB and NOB activity reach pseudo steady state. The model shows the ratio of μ_{AOB} to
264 μ_{NOB} increases in the intermittent aeration, compared to the ratio of μ_{max}^{AOB} to μ_{max}^{NOB} in continuous aeration
265 (1.5 ± 0.15 versus 1.1). AOB preferentially utilize oxygen to support growth while NOB are outcompeted or
266 their activity is suppressed.

267 To assess the relative contribution of DO/pH effects on NOB suppression, individual factors influencing
268 growth rates were calculated spatially (at different biofilm depths) and temporally (at different times in the
269 cycle). Considering the effective DO penetration depth, only results in the first 100- μm at the biofilm base
270 are shown (Figure 2B).

271 **DO Limitation in NOB Suppression**

272 O_2 is a growth substrate for both AOB and NOB. In counter-diffusion biofilms O_2 is provided via the lumen
273 and NH_4^+ via the bulk. In the biofilm, DO penetrates only 60 μm during aeration periods with the highest
274 concentration at the membrane-biofilm interface (biofilm depth= 0 μm), presenting spatial variations (Figure

275 S5A). Besides, DO varies over time during aeration cycles. DO at the membrane-biofilm interface is 0 mg/L
276 at the onset of aeration and quickly increases to the maximum concentration within 15 minutes. Afterwards,
277 DO concentrations within the biofilm remain stable until the end of aeration.

278 The DO limitation effect was evaluated based on oxygen concentrations within the biofilm (Figure 2B, 1-
279 DO limitation). In aeration periods, during the first 15 minutes DO strongly limits both AOB and NOB
280 activities. During the following period, the limitation is alleviated as DO increases and stabilizes, but still
281 remains strong above 30 μm . With a lower DO affinity NOB are more oxygen-limited than AOB. However,
282 the relatively stronger limitation to NOB is insignificant in its suppression. Model results show that oxygen
283 transfer and its diffusion mostly affects NH_4^+ oxidation efficiency rather than nitrification efficiency (Table
284 S7).

285 **pH-enzyme Effect on NOB Suppression**

286 Because pH affects AOB/NOB kinetics directly and indirectly, it is necessary to incorporate pH effects in
287 models.^{14,37} Here MSNBM predicts local pH values within the biofilm and the response to transient aeration
288 phases (Figure S5B). While measurements showed that bulk pH remained relatively stable (± 0.2), pH within
289 the biofilm, especially in the DO-penetrated zone, showed considerable variations (± 0.6). At the onset of
290 aeration the model indicates a transient pH upshift at the biofilm base (0-15 minutes). The accumulated
291 alkalinity is attributed to continuous CO_2 diffusion from the biofilm base to the membrane lumen where N_2
292 gas flows through in the previous non-aeration period and slight denitrification activities. As aeration
293 continues, pH decreases due to proton production associated with NH_4^+ oxidation. Simulations predict that
294 pH within the biofilm becomes lower than in the bulk after 1-hour aeration and decreases slowly afterwards.
295 At the end of aeration pH at the biofilm base is 0.4 units lower than the average bulk pH, which will increase
296 again in the following non-aerated phase. Thus pH varies periodically in the intermittently aerated biofilms,
297 a pattern similar but slower than DO variations.

298 The pH-enzyme effect was assessed based on local pH values (Figure 2B, 2- pH-enzyme effect). It favors
299 NOB growth over AOB as NOB have a lower pH_{opt} (NOB: 7.7 versus AOB: 8.4) and pH varies in the
300 optimal range for its growth. Moreover, the pH-enzyme effect is also insignificant in the overall AOB/NOB

301 competition due to their robust growth in broad pH ranges and the relatively small pH variations in the
302 system.

303 **pH Substrate-speciation Effects on NOB Suppression**

304 FA/FNA concentrations rely on pH values as well as total $\text{NH}_4^+/\text{NO}_2^-$ concentrations. In counter-diffusion
305 biofilms, NH_4^+ , provided via the bulk, is oxidized at the biofilm base producing NO_2^- which diffuses
306 backward into the bulk.¹⁰ Based on ionic N concentrations, FA and FNA speciation synchronizes with pH
307 variations (Figure S5C and S5D). For instance, at the onset of aeration FA concentration is high due to NH_4^+
308 and alkalinity accumulation from the previous non-aeration period. During the following aeration period, FA
309 concentration decreases, as pH drops and NH_4^+ consumption continues. On the other hand, FNA shows
310 reversed variations: increasing as aeration progresses and with biofilm depth as a result of the proton and
311 NO_2^- production.

312 The pH substrate-speciation effect was assessed based on FA/FNA concentrations within the biofilm (Figure
313 2B, 3- FA/FNA inhibition). During the first 15 minutes, FA strongly inhibits AOB/NOB microbial activities
314 ($\text{FA} > K_{I,FA}$). Afterwards, the inhibition is alleviated as FA decreases. Noticeably, FA inhibits AOB and
315 NOB in different ways: the inhibition effect remains strong for NOB throughout the aeration period (from
316 0.26 to 0.62), while it obviously weakens for AOB (from 0.54 to 0.89). FA inhibition rapidly becomes the
317 most determinant factor in suppressing NOB over AOB. As FNA concentrations are always an order of
318 magnitude lower than $K_{I,FNA}$, its inhibition effect on microbial activities is always minor thereby contributing
319 little to NOB suppression.

320 Besides the inhibitor effect ($K_I/(K_I + S)$), FA/FNA exhibit the substrate limitation effect ($S/(K_S + S)$) in
321 biological processes (Equation 2). However, FA and FNA concentrations are far above the substrate
322 affinities (K_{FA}^{AOB} and K_{FNA}^{NOB}) in the system, making the substrate limitation effects negligible.

323 Overall, FA inhibition caused by pH substrate-speciation is the crucial factor in suppressing NOB in the
324 intermittently aerated biofilm reactors. Nitrification success is insensitive to oxygen affinity constants or DO
325 concentrations at the membrane-biofilm interface- a conclusion different from previous studies.^{38,39} Downing
326 and Nerenberg²² suggested manipulating interface DO as an effective method to control shortcut nitrification

327 in MABRs: with a lower interface DO, more NO_2^- accumulated. However, their biofilms performed at low
328 nitrification rates with a low influent NH_4^+ concentration- 3 mg-N/L, suggesting little FA inhibition and no
329 NO_2^- accumulation or significant pH gradients. The single DO gradient within the biofilm present the
330 interface DO as a key role in nitrification success. This method might not apply for N-rich wastewater
331 treatment. For example Lackner and Smets³⁶ concluded that nitrification success based only on interface DO
332 was not possible in a counter-diffusion biofilm with high influent NH_4^+ concentrations (20-800 mg-N/L), and
333 nitrification efficiency was not predicted from oxygen affinity constants.

334 Counter- and co-diffusion biofilms have different mechanisms of NOB suppression due to different spatial
335 structures and population distributions.^{32,35,36} In counter-diffusion biofilms, the theoretically optimal habitat
336 for NOB is the biofilm base, where both $S_{\text{O}_2}/K_{\text{O}_2}$ and $S_{\text{FNA}}/K_{\text{FNA}}$ have the highest values. By contrast, the
337 base is not the optimal for AOB growth, as $S_{\text{O}_2}/K_{\text{O}_2}$ and $S_{\text{FA}}/K_{\text{FA}}$ cannot have the maximum at the same
338 spatial position. Outcompeting NOB can be more difficult in counter-diffusion over co-diffusion biofilms,
339 where microbes (AOB and NOB) share the optimal habitats at the biofilm top near the biofilm/liquid
340 interphase. Others have similarly observed that NOB could survive better in counter- versus co- diffusion
341 biofilms, even when operated under constant oxygen limited ($\text{DO} < 0.1$ mg/L) and high pH (8.0-8.3)
342 conditions in the bulk.³² The inherent system geometry of membrane-aerated biofilms complicates NOB
343 inhibition/washout. Besides, when applying intermittent aeration, periodic pH variations at the biofilm base
344 exert a significant effect on NOB dynamics in counter-diffusion biofilms because of continuous CO_2
345 diffusion to the gas lumen. However, such pH variations are not expected in co-diffusion biofilms. Many
346 studies have highlighted the benefits of low DO with high FA to maintain shortcut NH_4^+ removal in co-
347 diffusion biofilms.^{17,40} Park et al.³ explored simultaneous effects of DO and FA/FNA in lab-scale co-
348 diffusion nitrifying biofilms, and found that NO_2^- accumulated due to DO limitation or FA inhibition and
349 long-term NOB suppression could not be maintained without DO limitation involved. The results were
350 consistent with Brockmann and Morgenroth⁴¹ who suggested that oxygen limitation was the main
351 mechanism for NOB suppression and FA inhibition was not necessarily required in co-diffusion biofilms.
352 However, DO limitation in nitrification counter-diffusion biofilms appears not as significant as reported for co-

353 diffusion biofilms, consistent with the observation that nitrification could not be achieved by solely
354 manipulating air pressure in the membrane lumen in MABRs.²¹

355 **3.3 Potential explanation of NOB Suppression in the study of Pellicer-Nàcher et al. (2010)**

356 To answer why NO₂⁻ accumulated after switching from continuous to intermittent aeration in MABRs,
357 simulations were carried out with the calibrated MSNBM in continuous aeration for 200 days followed by
358 intermittent aeration (6-hour aeration and 6-hour non-aeration cycles). The simulation shows a nitrifying
359 biofilm during continuous aeration (NE = 0%) indicating no NOB suppression (Table 2- continuous
360 aeration). After switching to intermittent aeration the model predicts NOB suppression- NO₃⁻ decrease and
361 NE increase (Table 2- strategy A, Figure S6). To find the critical factor for NOB suppression, variations of
362 individual pH/DO effect on AOB/NOB competition were assessed: each effect $\frac{effect_{AOB}}{effect_{NOB}}$ in intermittent
363 aeration (for instance at day 215) was normalized by its value during continuous aeration. A value higher
364 than 1 means the effect favors NOB suppression in intermittent aeration, and lower than 1 that it favors NOB
365 growth.

366 Only FA inhibition is identified to favor NO₂⁻ accumulation after switching the aeration strategy, while DO
367 limitation, pH-enzyme effect and FNA inhibition remain unchanged (Figure S7). FA inhibition shows certain
368 varying patterns in intermittent aeration: (1) it is overall enhanced due to an increased residual NH₄⁺; (2) it is
369 particularly strong during the first 15 minutes of aeration. The simulated increase of residual NH₄⁺ after
370 changing to intermittent aeration was also observed in the study of Pellicer-Nàcher et al.:²¹ in reactor B bulk
371 NH₄⁺ increased by 100 mg/L at stage 1 and 2 (intermittent aeration) compared to stage 0 (continuous
372 aeration). Compared to continuous aeration, MABRs in intermittent aeration display a tradeoff between
373 NH₄⁺ removal efficiency and nitrification efficiency (Table 2). Nitrification is assisted by the evaluated residual
374 NH₄⁺, which underlines the importance of a minimum NH₄⁺ concentration in the bulk. Pérez et al.¹⁸ also
375 highlighted the need for minimum residual NH₄⁺ for NOB suppression in co-diffusion biofilms, but
376 attributed the nitrification success to differential oxygen limitation rather than FA inhibition- as NOB were
377 outcompeted due to the strong oxygen limiting conditions imposed by a high residual NH₄⁺. The strong FA
378 inhibition at the onset of aeration is due to pH upshifts at the biofilm base in the previous anoxic phases. It

379 causes a longer lag phase of NOB activity over AOB, which could be another reason in the nitrification
380 success. Theoretically, NOB locate at the biofilm base, if enriched in MABRs, thus pH upshift at the base is
381 more efficient to prompt FA inhibition than increasing bulk pH. This lag phase has also been observed in
382 other intermittently aerated systems.^{42,43} Kornaros et al.⁴⁴ and Gilbert et al.⁴⁵ attributed the lag phase to a long
383 (enzyme) reactivation time in NOB nitrogen metabolism after anoxic exposure in batch continuous stirred-
384 tank reactors. However, the possibility for pH variations was not considered in those studies, even though
385 CO₂ stripping could slowly increase bulk pH.⁴⁶

386 **3.4 Nitrification in Various Intermittent Aeration Strategies**

387 For an intermittent aeration system with certain NH₄⁺/O₂ surface loadings, the aeration duration determines
388 residual NH₄⁺ concentrations: a longer aeration lowers residual NH₄⁺. The aeration intermittency determines
389 pH upshift times and the variation range of bulk concentrations: a higher frequency causes more pH upshifts
390 and a narrow variation range. This information can be utilized to optimize intermittent aeration strategies for
391 efficient nitrification in MABRs (Table 2). MSNBM simulation shows that a higher aeration intermittency can
392 accelerate NOB suppression (A and C) due to more times of pH upshift in non-aeration phases to retard
393 NOB activity while slightly affecting AOB activity, or decelerate NOB suppression (B and A) due to the
394 relatively high bulk NH₄⁺ (pH) at the onset of aeration phases even the averaged bulk concentrations are the
395 same. Longer aeration duration (D) leads to a slower nitrification process but a higher NH₄⁺ removal efficiency,
396 while keeping the same aeration intermittency. It is consistent with the observation in Mota et al.⁴⁷ that
397 intermittently aerated reactors with longer anoxic phase had the lower NOB abundance and relatively higher
398 NH₄⁺ effluent concentrations. Both studies suggest that the maximum aeration duration should be set to
399 ensure nitrification success in intermittent aeration, and a specific to the treated wastewater ratio of aeration to
400 non-aeration phase is needed to balance NOB suppression against NH₄⁺ removal.⁴⁸ Simulation with high
401 NH₄⁺ concentrations predicts fast nitrification in the intermittent aeration (E), and vice versa slow nitrification
402 with low influent NH₄⁺ (F). Further simulation with low NH₄⁺ concentrations but high bulk pH (G) shows
403 efficient nitrification, confirming a key factor in NOB suppression was bulk FA rather than residual NH₄⁺
404 (more simulations in Table S8). In an intermittent aeration regime, the bulk FA can provide a rapid indicator

405 of the nitrification potential of MABRs (Figure S10). It reveals that aeration duration and aeration
406 intermittency are two key criteria that affect nitrification efficiency in MABRs at a certain influent loading.

407 In conclusion, we provide experimental evidence that intermittent aeration supports efficient nitrification in
408 membrane aerated biofilm reactors (MABRs). A pH-explicit 1-D multispecies nitrifying biofilm model
409 (MSNBM) is developed and calibrated: model analysis reveals that NOB suppression - associated with
410 intermittent aeration - is primarily governed by *periodic* FA inhibition as the consequence of transient pH
411 upshifts during non-aeration. These pH upshifts are mainly caused by alkalinity increases due to CO₂
412 stripping to the membrane lumen (which also occurs during aeration) *plus* the cessation of proton production
413 (which only occurs during aeration). In counter diffusion biofilms pH effect is more important than DO
414 (limitation) effect on NOB suppression. Both aeration intermittency and duration are effective control factors
415 to obtain nitrification success in intermittently membrane-aerated biofilms, and maintaining nitrification and
416 NH₄⁺ removal efficiency is more easily ensured if operated with high buffer capacities.

417 **Acknowledgement**

418 The authors would like to thank the China Scholarship Council (CSC) for financial support to Yunjie Ma,
419 and the Innovation Fund Denmark (IFD) (Project LaGAS, File No. 0603-00523B) for additional financial
420 support.

421

422 **References**

- 423 (1) Hellinga, C.; Schellen, A.; Mulder, J.; Vanloosdrecht, M.; Heijnen, J. The sharon process: An
 424 innovative method for nitrogen removal from ammonium-rich waste water. *Water Sci. Technol.* **1998**,
 425 37 (9), 135–142.
- 426 (2) Jenicek, P.; Svehla, P.; Zabranska, J.; Dohanyos, M. Factors affecting nitrogen removal by
 427 nitrification/denitrification. *Water Sci. Technol.* **2004**, 49 (5–6), 73–79.
- 428 (3) Park, S.; Chung, J.; Rittmann, B. E.; Bae, W. Nitrite accumulation from simultaneous free-ammonia
 429 and free-nitrous-acid inhibition and oxygen limitation in a continuous-flow biofilm reactor.
 430 *Biotechnol. Bioeng.* **2015**, 112 (1), 43–52.
- 431 (4) van Dongen, U.; Jetten, M. S.; van Loosdrecht, M. C. The SHARON-Anammox process for treatment
 432 of ammonium rich wastewater. *Water Sci. Technol.* **2001**, 44 (1), 153–160.
- 433 (5) Kuenen, J. G. Anammox bacteria: from discovery to application. *Nat. Rev. Microbiol.* **2008**, 6 (4),
 434 320–326.
- 435 (6) Sliemers, A. O.; Haaijer, S. C. M.; Stafsnes, M. H.; Kuenen, J. G.; Jetten, M. S. M. Competition and
 436 coexistence of aerobic ammonium- and nitrite-oxidizing bacteria at low oxygen concentrations. *Appl.*
 437 *Microbiol. Biotechnol.* **2005**, 68 (6), 808–817.
- 438 (7) Vadivelu, V. M.; Yuan, Z.; Fux, C.; Keller, J. The inhibitory effects of free nitrous acid on the energy
 439 generation and growth processes of an enriched *Nitrobacter* culture. *Environ. Sci. Technol.* **2006**, 40
 440 (14), 4442–4448.
- 441 (8) Terada, A.; Lackner, S.; Kristensen, K.; Smets, B. F. Inoculum effects on community composition
 442 and nitrification performance of autotrophic nitrifying biofilm reactors with counter-diffusion geometry.
 443 *Environ. Microbiol.* **2010**, 12 (10), 2858–2872.
- 444 (9) Fux, C.; Huang, D.; Monti, A.; Siegrist, H. Difficulties in maintaining long-term partial nitrification of
 445 ammonium-rich sludge digester liquids in a moving-bed biofilm reactor (MBBR). *Water Sci. Technol.*
 446 **2004**, 49 (11–12), 53–60.
- 447 (10) Schramm, A.; De Beer, D.; Gieseke, A.; Amann, R. Microenvironments and distribution of nitrifying
 448 bacteria in a membrane-bound biofilm. *Environ. Microbiol.* **2000**, 2 (6), 680–686.
- 449 (11) Shanahan, J. W.; Semmens, M. J. Alkalinity and pH effects on nitrification in a membrane aerated
 450 bioreactor: An experimental and model analysis. *Water Res.* **2015**, 74, 10–22.
- 451 (12) Vannecke, T. P. W.; Volcke, E. I. P. Modelling microbial competition in nitrifying biofilm reactors.
 452 *Biotechnol. Bioeng.* **2015**, 112 (12), 2550–2561.
- 453 (13) Park, S.; Bae, W.; Chung, J.; Baek, S.-C. Empirical model of the pH dependence of the maximum
 454 specific nitrification rate. *Process Biochem.* **2007**, 42 (12), 1671–1676.
- 455 (14) Fumasoli, A.; Morgenroth, E.; Udert, K. M. Modeling the low pH limit of *Nitrosomonas eutropha* in
 456 high-strength nitrogen wastewaters. *Water Res.* **2015**, 83, 161–170.
- 457 (15) Carrera, J.; Jubany, I.; Carvallo, L.; Chamy, R.; Lafuente, J. Kinetic models for nitrification inhibition
 458 by ammonium and nitrite in a suspended and an immobilised biomass systems. *Process Biochem.*
 459 **2004**, 39 (9), 1159–1165.
- 460 (16) Martin, K. J.; Picioreanu, C.; Nerenberg, R. Assessing microbial competition in a hydrogen-based
 461 membrane biofilm reactor (MBfR) using multidimensional modeling. *Biotechnol. Bioeng.* **2015**, 112
 462 (9), 1843–1853.
- 463 (17) Park, S.; Bae, W.; Rittmann, B. E. Multi-species nitrifying biofilm model (MSNBM) including free
 464 ammonia and free nitrous acid inhibition and oxygen limitation. *Biotechnol. Bioeng.* **2010**, 105 (6),
 465 1115–1130.

- 466 (18) Pérez, J.; Lotti, T.; Kleerebezem, R.; Picioreanu, C.; van Loosdrecht, M. C. M. Outcompeting nitrite-oxidizing bacteria in single-stage nitrogen removal in sewage treatment plants: A model-based study. *Water Res.* **2014**, *66*, 208–218.
- 467
- 468
- 469 (19) Casey, E.; Glennon, B.; Hamer, G. Review of membrane aerated biofilm reactors. *Resour. Conserv. Recycl.* **1999**, *27* (1–2), 203–215.
- 470
- 471 (20) Terada, A.; Yamamoto, T.; Igarashi, R.; Tsuneda, S.; Hirata, A. Feasibility of a membrane-aerated biofilm reactor to achieve controllable nitrification. *Biochem. Eng. J.* **2006**, *28* (2), 123–130.
- 472
- 473 (21) Pellicer-Nàcher, C.; Sun, S.; Lackner, S.; Terada, A.; Schreiber, F.; Zhou, Q.; Smets, B. F. Sequential aeration of membrane-aerated biofilm reactors for high-rate autotrophic nitrogen removal: experimental demonstration. *Environ. Sci. Technol.* **2010**, *44* (19), 7628–7634.
- 474
- 475
- 476 (22) Downing, L. S.; Nerenberg, R. Effect of oxygen gradients on the activity and microbial community structure of a nitrifying, membrane-aerated biofilm. *Biotechnol. Bioeng.* **2008**, *101* (6), 1193–1204.
- 477
- 478 (23) Gieseke, A.; Beer, D. De. Use of microelectrodes to measure in situ microbial activities in biofilms, sediments, and microbial mats. *Mol. Microb. Ecol. Man.* **2004**, *2*, 1281–1612.
- 479
- 480 (24) Terada, A.; Lackner, S.; Tsuneda, S.; Smets, B. F. Redox-stratification controlled biofilm (ReSCoBi) for completely autotrophic nitrogen removal: the effect of co- versus counter-diffusion on reactor performance. *Biotechnol. Bioeng.* **2007**, *97* (1), 40–51.
- 481
- 482
- 483 (25) Reichert, P. AQUASIM 2.0—Computer program for the identification and simulation of aquatic systems. *Dubendorf, Switz. EAWAG.* **1998**.
- 484
- 485 (26) Hiatt, W. C.; Grady, C. P. L. An updated process model for carbon oxidation, nitrification, and denitrification. *Water Environ. Res.* **2008**, *80*, 2145–2156.
- 486
- 487 (27) Blackburne, R.; Yuan, Z.; Keller, J. Demonstration of nitrogen removal via nitrite in a sequencing batch reactor treating domestic wastewater. *Water Research.* 2008, pp 2166–2176.
- 488
- 489 (28) Sötemann, S.; Musvoto, E.; Wentzel, M.; Ekama, G. Integrated biological, chemical and physical processes kinetic modelling
Part 1 – Anoxic-aerobic C and N removal in the activated sludge system. *Water SA* **2006**, *31* (4), 1044–1062.
- 490
- 491
- 492 (29) Van Hulle, S. W. H.; Volcke, E. I. P.; Teruel, J. L.; Donckels, B.; van Loosdrecht, M. C. M.; Vanrolleghem, P. A. Influence of temperature and pH on the kinetics of the Sharon nitrification process. *J. Chem. Technol. Biotechnol.* **2007**, *82* (5), 471–480.
- 493
- 494
- 495 (30) Musvoto, E. V.; Wentzel, M. C.; Loewenthal, R. E.; Ekama, G. A. Integrated chemical-physical processes modelling - I. Development of a kinetic-based model for mixed weak acid/base systems. *Water Res.* **2000**, *34* (6), 1857–1867.
- 496
- 497
- 498 (31) Hao, X.; Heijnen, J. J.; Van Loosdrecht, M. C. . Model-based evaluation of temperature and inflow variations on a partial nitrification–ANAMMOX biofilm process. *Water Res.* **2002**, *36* (19), 4839–4849.
- 499
- 500
- 501 (32) Wang, R.; Terada, A.; Lackner, S.; Smets, B. F.; Henze, M.; Xia, S.; Zhao, J. Nitrification performance and biofilm development of co-and counter-diffusion biofilm reactors: modeling and experimental comparison. *Water Res.* **2009**, *43* (10), 2699–2709.
- 502
- 503
- 504 (33) Pellicer-Nàcher, C.; Domingo-Félez, C.; Lackner, S.; Smets, B. F. Microbial activity catalyzes oxygen transfer in membrane-aerated nitrifying biofilm reactors. *J. Memb. Sci.* **2013**, *446*, 465–471.
- 505
- 506 (34) Power, M. The predictive validation of ecological and environmental models. *Ecol. Modell.* **1993**, *68* (1–2), 33–50.
- 507
- 508 (35) Brockmann, D.; Rosenwinkel, K.-H.; Morgenroth, E. Practical identifiability of biokinetic parameters of a model describing two-step nitrification in biofilms. *Biotechnol. Bioeng.* **2008**, *101* (3), 497–514.
- 509
- 510 (36) Lackner, S.; Smets, B. F. Effect of the kinetics of ammonium and nitrite oxidation on nitrification

- 511 success or failure for different biofilm reactor geometries. *Biochem. Eng. J.* **2012**, *69*, 123–129.
- 512 (37) Vangsgaard, A. K.; Mauricio-Iglesias, M.; Valverde-Pérez, B.; Gernaey, K. V.; Sin, G. pH variation
513 and influence in an autotrophic nitrogen removing biofilm system using an efficient numerical
514 solution strategy. *Water Sci. Technol.* **2013**, *67* (11), 2608.
- 515 (38) Wyffels, S.; Van Hulle, S. W. H.; Boeckx, P.; Volcke, E. I. P.; Cleemput, O. Van; Vanrolleghem, P.
516 A.; Verstraete, W. Modeling and simulation of oxygen-limited partial nitrification in a membrane-
517 assisted bioreactor (MBR). *Biotechnol. Bioeng.* **2004**, *86* (5), 531–542.
- 518 (39) Volcke, E. I. P.; Sanchez, O.; Steyer, J.-P.; Dabert, P.; Bernet, N. Microbial population dynamics in
519 nitrifying reactors: Experimental evidence explained by a simple model including interspecies
520 competition. *Process Biochem.* **2008**, *43* (12), 1398–1406.
- 521 (40) Chung, J.; Bae, W.; Lee, Y.-W.; Rittmann, B. E. Shortcut biological nitrogen removal in hybrid
522 biofilm/suspended growth reactors. *Process Biochem.* **2007**, *42* (3), 320–328.
- 523 (41) Brockmann, D.; Morgenroth, E. Evaluating operating conditions for outcompeting nitrite oxidizers
524 and maintaining partial nitrification in biofilm systems using biofilm modeling and Monte Carlo
525 filtering. *Water Res.* **2010**, *44* (6), 1995–2009.
- 526 (42) Yoo, H.; Ahn, K.-H.; Lee, H.-J.; Lee, K.-H.; Kwak, Y.-J.; Song, K.-G. Nitrogen removal from
527 synthetic wastewater by simultaneous nitrification and denitrification (SND) via nitrite in an
528 intermittently-aerated reactor. *Water Res.* **1999**, *33* (1), 145–154.
- 529 (43) Gilbert, E. M.; Agrawal, S.; Brunner, F.; Schwartz, T.; Horn, H.; Lackner, S. Response of Different
530 Nitrospira Species To Anoxic Periods Depends on Operational DO. *Environ. Sci. Technol.* **2014**, *48*
531 (5), 2934–2941.
- 532 (44) Kornaros, M.; Dokianakis, S. N.; Lyberatos, G. Partial Nitrification/Denitrification Can Be Attributed
533 to the Slow Response of Nitrite Oxidizing Bacteria to Periodic Anoxic Disturbances. *Environ. Sci.*
534 *Technol.* **2010**, *44* (19), 7245–7253.
- 535 (45) Gilbert, E. M.; Agrawal, S.; Brunner, F.; Schwartz, T.; Horn, H.; Lackner, S. Response of Different
536 Nitrospira Species To Anoxic Periods Depends on Operational DO. *Environ. Sci. Technol.* **2014**, *48*
537 (5), 2934–2941.
- 538 (46) Li, J.; Elliott, D.; Nielsen, M.; Healy, M. G.; Zhan, X. Long-term partial nitrification in an
539 intermittently aerated sequencing batch reactor (SBR) treating ammonium-rich wastewater under
540 controlled oxygen-limited conditions. *Biochem. Eng. J.* **2011**, *55* (3), 215–222.
- 541 (47) Mota, C.; Head, M. A.; Ridenoure, J. A.; Cheng, J. J.; de los Reyes, F. L. Effects of Aeration Cycles
542 on Nitrifying Bacterial Populations and Nitrogen Removal in Intermittently Aerated Reactors. *Appl.*
543 *Environ. Microbiol.* **2005**, *71* (12), 8565–8572.
- 544 (48) Kornaros, M.; Marazioti, C.; Lyberatos, G. A pilot scale study of a sequencing batch reactor treating
545 municipal wastewater operated via the UP-PND process. *Water Sci. Technol.* **2008**, *58* (2), 435–438.
- 546
- 547

548 **Table 1.** Kinetic parameter values of AOB and NOB in the calibrated model.

Kinetic parameters	AOB	NOB	References
μ_{max} : the maximum specific growth rate, 1/d	2.35 ^{2.72} ¹	2.15 ^{1.75} ¹	this study
K_{O_2} : half-saturation coefficient for O ₂ , mg/L	0.6	1.2	Hiatt and Grady ²⁶
Y : autotrophic yield, mgCOD/mgN	0.18	0.06	Hiatt and Grady ²⁶
$K_{FA}^{AOB}, K_{FNA}^{NOB}$: half-saturation coefficient, mg/L	0.0075	0.0001	Hiatt and Grady ²⁶
$K_{I,FA}$: free ammonia inhibition coefficient, mg/L	1	0.2	Hiatt and Grady ²⁶
$K_{I,FNA}$: free nitrous acid inhibition coefficient, mg/L	0.1	0.04	Hiatt and Grady ²⁶
b_{max} : decay coefficient, 1/d	0.17	0.073	Hao et al. ³¹
pH _{opt} (ω): optimal pH	8.4(3.2)	7.7(2.4)	Park et al. ¹³

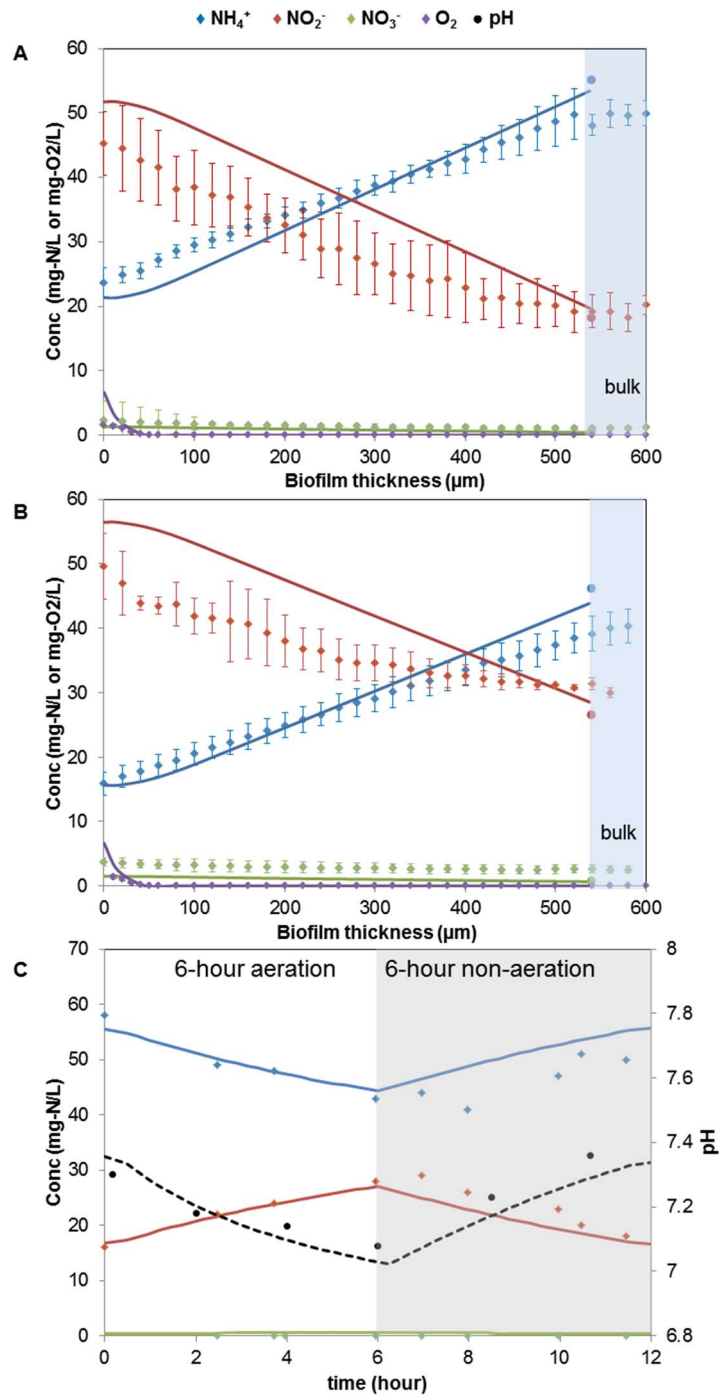
549 ¹default growth rates in ASMN with temperature correction (33°C)

550

551 **Table 2.** Predicted nitrification efficiencies (NE, %) in various intermittent aeration strategies

Simulation Case	Influent ²		Effluent (Bulk)			
	NH ₄ ⁺ _{in} (mg-N/L)	Buffer capacity ²	NH ₄ ⁺ (mg-N/L)	pH	FA ³ (mg-N/L)	NE _{normalized} ⁴
continuous	75	2.1	39	6.96	0.27	0.01
A: 6+6 ¹	75	2.1	53.0 ± 5	7.23 ± 0.15	0.71	1.00 ⁴
B: 1+1	75	2.1	52.5 ± 1	7.22 ± 0.02	0.69	0.73
C: 12+12	75	2.1	53.1 ± 10	7.25 ± 0.25	0.78	0.79
D: 8+4	75	2.1	47.8 ± 4	7.14 ± 0.15	0.52	0.41
E: 6+6	100	2.1	72.0 ± 7	7.25 ± 0.15	1.02	1.74
F: 6+6	50	2.1	35.0 ± 3	7.20 ± 0.15	0.45	0.21
G: 6+6	50	5	31.2 ± 5	7.41 ± 0.10	0.64	0.83

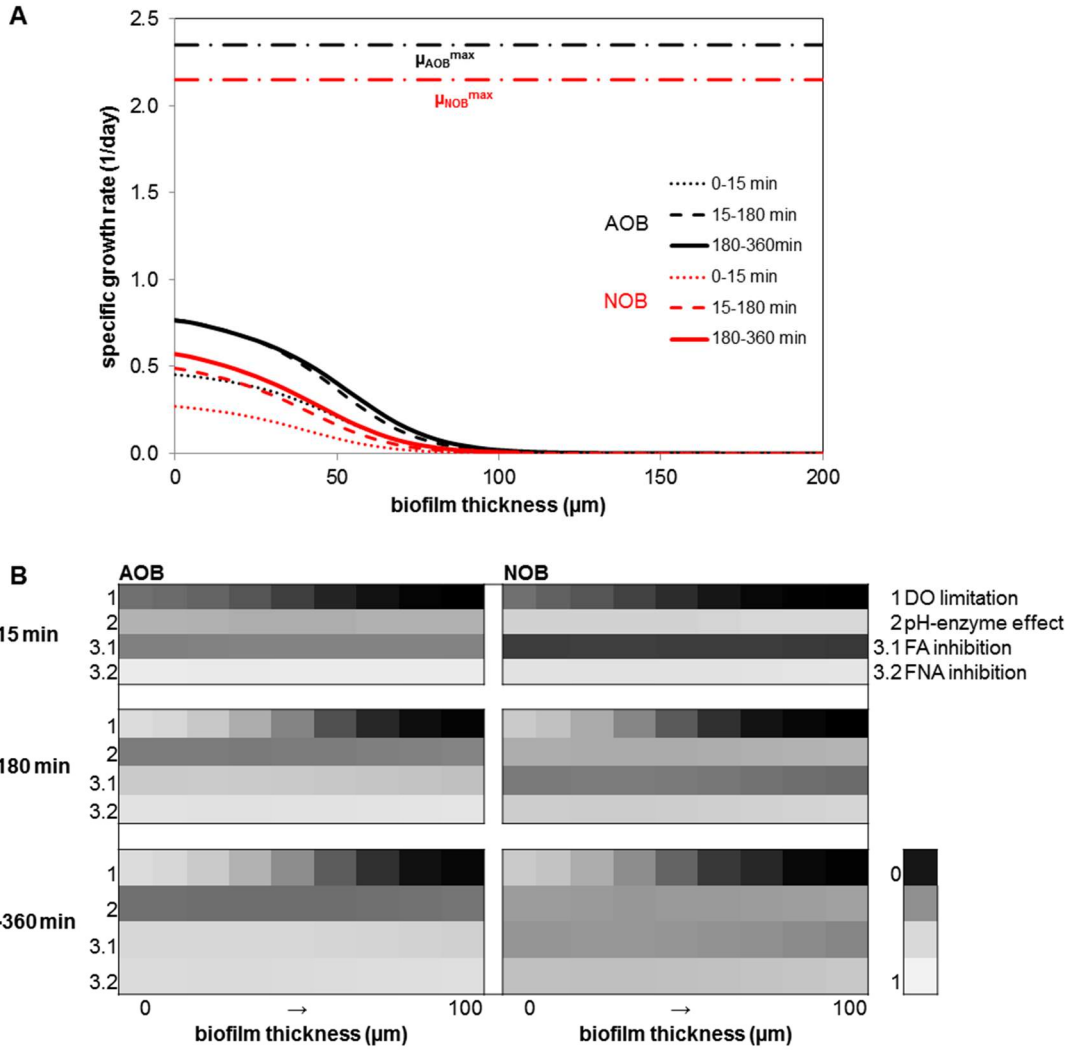
552 ¹Aeration strategy 6+6 meant a 12-hour intermittent aeration cycle consisting of a 6-hour aeration phase and
553 a 6-hour non-aeration phase. ²Buffer capacity in the influent was recorded as the molar ratio of bicarbonate
554 (HCO₃⁻) to ammonium (NH₄⁺_N). ³FA was calculated with the averaged NH₄⁺ concentrations and bulk pH
555 during a full aeration cycle (equation 6). ⁴For a clear comparison, NE was normalized to the Nitrification
556 efficiency in the default simulation case A (NE = 48.5%). MSNBM was run in continuous aeration (200 days)
557 to achieve a mature nitrifying biofilm, followed by various intermittent aeration strategies: (A-D) different
558 intermittent aeration but the same influent; (A,E-G) the same aeration intermittency but different influent
559 concentrations. NEs in the NOB suppression process in intermittent aeration were recorded (e.g. at day 215)
560 (Table S6). In simulations E-G, oxygen loadings proportionally varied with NH₄⁺ influent concentrations
561 (more simulations in Table S8).



562

563 **Figure 1.** Experimental (discrete symbols) and predicted (line) concentrations in MABR at steady state (A)
 564 microprofiles in the first aeration hour, (B) microprofiles in the last aeration hour, and (C) bulk profiles in a
 565 12-hour intermittent aeration cycle. For each micro profile, replicates ($n>3$) were made and the average was
 566 shown.

567

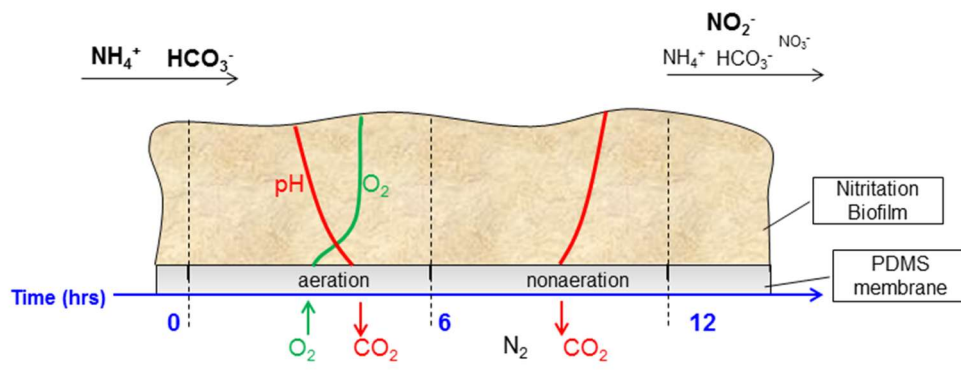


568

569 **Figure 2.** A- Specific growth rates of AOB and NOB within the biofilm in a 6-hour aeration period at day 15
 570 (AOB- black, NOB- red). B- Individual effect on AOB and NOB within the 100 μm -aerated biofilm base in a
 571 6-hour aeration period at day 15. (0- strong limitation/inhibition effect, 1- no limitation/inhibition effect)

572

573



574

575

TOC- Graphical abstract